THE JOURNAL OF BIOLOGICAL CHEMISTRY VOL. 284, NO. 22, pp. 14914–14920, May 29, 2009


# The Novel S527F Mutation in the Integrin β3 Chain Induces a High Affinity αIIbβ3 Receptor by Hindering Adoption of the Bent Conformation*

Received for publication, December 5, 2008, and in revised form, March 26, 2009 Published, JBC Papers in Press, March 27, 2009, DOI 10.1074/jbc.M809167200

**Karen Vanhoorelbeke[‡1,2], Simon F. De Meyer[‡1], Inge Pareyn[‡], Chantal Melchior[§], Sebastien Plançon[§], Christiane Margue[§], Olivier Pradier[¶], Pierre Fondu[‖], Nelly Kieffer[§], Timothy A. Springer[**], and Hans Deckmyn[‡]**

*From the [‡]Laboratory for Thrombosis Research, Interdisciplinary Research Center, Katholieke Universiteit Leuven Campus Kortrijk, 8500 Kortrijk, Belgium, the [§]Laboratoire de Biologie et Physiologie Intégrée (CNRS/GDRE-ITI), Université du Luxembourg, L-1511 Luxembourg, the [¶]Hôpital Erasme and [‖]Centre Hospitalier Universitaire Brugmann, Université Libre de Bruxelles, 1050 Brussels, Belgium, and the **Immune Disease Institute, Harvard Medical School, Boston, Massachusetts 02115*

**Three heterozygous mutations were identified in the genes encoding platelet integrin receptor αIIbβ3 in a patient with an ill defined platelet disorder: one in the β3 gene (S527F) and two in the αIIb gene (R512W and L841M). Five stable Chinese hamster ovary cell lines were constructed expressing recombinant αIIbβ3 receptors bearing the individual R512W, L841M, or S527F mutation; both the R512W and L841M mutations; or all three mutations. All receptors were expressed on the cell surface, and mutations R512W and L841M had no effect on integrin function. Interestingly, the β3 S527F mutation produced a constitutively active receptor. Indeed, both fibrinogen and the ligand-mimetic antibody PAC-1 bound to non-activated αIIbβ3 receptors carrying the S527F mutation, indicating that the conformation of this receptor was altered and corresponded to the high affinity ligand binding state. In addition, the conformational change induced by S527F was evident from basal anti-ligand-induced binding site antibody binding to the receptor. A molecular model bearing this mutation was constructed based on the crystal structure of αIIbβ3 and revealed that the S527F mutation, situated in the third integrin epidermal growth factor-like (I-EGF3) domain, hindered the αIIbβ3 receptor from adopting a wild type-like bent conformation. Movement of I-EGF3 into a cleft in the bent conformation may be hampered both by steric hindrance between Phe[527] in β3 and the calf-1 domain in αIIb and by decreased flexibility between I-EGF2 and I-EGF3.**

The platelet receptor αIIbβ3 belongs to the family of integrin receptors that consist of noncovalently linked α/β-heterodimers. They are cell-surface receptors that play a role in cell-cell and cell-matrix interactions. Under resting conditions, integrin receptors adopt the low affinity conformation and do not interact with their ligands. Inside-out signaling turns the receptor into a high affinity conformation capable of ligand binding. Ligand binding itself induces additional conformational changes resulting in exposure of neoantigenic sites called ligand-induced binding sites (LIBS)[3] and generates in turn outside-in signaling, which triggers a range of downstream signals (1, 2).

Integrin αIIbβ3 is expressed on platelets and megakaryocytes. In flowing blood under resting conditions, αIIbβ3 does not interact with its ligand fibrinogen. When a blood vessel is damaged, platelets adhere at sites of vascular injury and become activated. As a consequence, αIIbβ3 adopts the high affinity conformation and binds fibrinogen. This results in platelet aggregation and thrombus formation, which eventually will stop the bleeding (3).

The topology of integrins comprises an extracellular, globular, N-terminal ligand-binding head domain (the β-propeller domain in the αIIb chain and the βI domain in the β3 chain) standing on two long legs or stalks (consisting of thigh, calf-1, and calf-2 domains in the αIIb chain and hybrid, plexin/semaphorin/integrin (PSI), four integrin endothelial growth factor-like (I-EGF), and β-tail domains in the β3 chain), followed by transmembrane and cytoplasmic domains (1, 2). X-ray crystal structures of the extracellular domain of non-activated αVβ3 revealed that the legs are severely bent, putting the head domain next to the membrane-proximal portions of the legs (4, 5). The bending occurs between I-EGF1 and I-EGF2 in the β-subunit and between the thigh and calf-1 domains in the α-subunit. This bent conformation represents the low affinity state of the receptor. The high affinity state of the receptor is induced by activation and is associated with a large-scale conformational rearrangement in which the integrin extends with a switchblade-like motion (2). Recently, the crystal structure of the entire extracellular domain of αIIbβ3 in its low affinity conformation was resolved and revealed that this integrin also adopts the bent conformation under resting conditions (6). Structural rearrangements in αIIbβ3 between the bent and

* This work was supported, in whole or in part, by National Institutes of Health Grant HL48675. This work was also supported by Katholieke Universiteit Leuven Grant GOA/2004/09 and European Union-RTN Grant HPRN-CT-2002-00253.

[1] Postdoctoral Fellow supported by the "Fonds voor Wetenschappelijk Onderzoek Vlaanderen" Belgium.

[2] To whom correspondence should be addressed: Lab. for Thrombosis Research, IRC, KU Leuven Campus Kortrijk, E. Sabbelaan 53, 8500 Kortrijk, Belgium. Tel.: 32-56-246019; Fax: 32-56-246997; E-mail: Karen.Vanhoorelbeke@kuleuven-kortrijk.be.

[3] The abbreviations used are: LIBS, ligand-induced binding site(s); PSI, plexin/semaphorin/integrin; I-EGF, integrin epidermal growth factor-like; FITC, fluorescein isothiocyanate; CHO, Chinese hamster ovary; WT, wild-type; DTT, dithiothreitol.

extended conformations are similar to what has been reported for other integrins (7).

We report here that the S527F mutation in the I-EGF3 region of the β3 polypeptide chain of the αIIbβ3 receptor induces a constitutively active receptor adopting an extended high affinity conformation. This was evidenced by spontaneous PAC-1, fibrinogen, and anti-LIBS antibody binding. These data were further corroborated by modeling the replacement of $Ser^{527}$ with Phe in the crystal structure of the extracellular domain of αIIbβ3. In this model, the S527F mutation decreases the flexibility of I-EGF3 and appears to prevent movement of the lower β-leg into the cleft between the upper β-leg and the lower α-leg. As a consequence, formation of the bent conformation of the non-activated receptor is hampered.

## EXPERIMENTAL PROCEDURES

*Case Report*—The propositus is a 20-year-old Arab male who has a clinical history of mild bleeding, including ecchymoses (spontaneously or after minimal injury) and epistaxis. However, circumcision and several dental extractions had been performed uneventfully and without the need for platelet transfusion. Laboratory diagnosis revealed that the Ivy bleeding time was moderately prolonged (14 min, 10 s). Maximal light transmission (with the difference between platelet-rich plasma and platelet-poor plasma set as 100%) obtained upon ADP-induced platelet aggregation was impaired (9 ± 6%, $n = 3$), whereas platelet aggregation in the presence of ristocetin was normal (84 ± 12%, $n = 3$). Platelet aggregation was performed with either 50 μmol/liter ADP (reference range of 64–100%; Roche Diagnostics, Mannheim, Germany) or 1.2 mg/ml ristocetin (reference range of 84–100%; Paesel Lorei GmbH & Co., Duisburg, Germany) using platelet-rich plasma. Unfortunately, as the patient was no longer available for further platelet studies, no clear diagnosis could be made.

*Antibodies*—Anti-human CD41 (anti-αIIb) and fluorescein isothiocyanate (FITC)-labeled rabbit anti-mouse antibodies were from Dako (Glostrup, Denmark); anti-AP3 (anti-β3) and anti-AP2 (anti-αIIbβ3) antibodies were from GTI Diagnostics (Wisconsin, WI). Anti-LIBS1 and anti-LIBS2 monoclonal antibodies were a kind gift of Dr. M. Ginsberg (The Scripps Research Institute, La Jolla, CA) (8, 9). FITC-labeled PAC-1 (10) was from BD Biosciences.

*Identification of Mutations in the αIIb and β3 Genes*—Genomic DNA was isolated from EDTA-anticoagulated blood of the patient using the QIAamp® DNA blood midi kit (Qiagen, Venlo, The Netherlands). A total of 40 pairs of oligonucleotides were used to amplify all 30 exons of the αIIb gene and 15 exons of the β3 gene with their intronic splicing signals. To obtain pure PCR products, $MgCl_2$ concentration and annealing temperature were optimized. Pure PCR products were directly sequenced (Genomex, Meylan, France).

*Preparation of Mutant αIIb and β3 DNA Constructs*—pcDNA3.1(−)NeoαIIb-WT and pcDNA3.1(−)Neoβ3-WT plasmids have been constructed previously (11) and were used as templates for mutagenesis. The primers used to introduce the desired mutations contained, in addition, a silent mutation creating a new restriction site for later identification of positive clones. This strategy resulted in three expression plasmids carrying the DNA coding for the R512W, L841M, and S527F mutations designated as pcDNA3.1(−)NeoαIIb-R512W, pcDNA3.1(−)NeoαIIb-L841M, and pcDNA3.1(−)Neoβ3-S527F, respectively.

To construct the pcDNA3.1(−)NeoαIIb plasmid with both the R512W and L841M mutations, the pcDNA3.1(−)NeoαIIb-R512W and pcDNA3.1(−)NeoαIIb-L841M plasmids were digested with NruI, and the insert from pcDNA3.1(−)NeoαIIb-R512W was ligated into the digested pcDNA3.1(−)NeoαIIb-L841M plasmid.

*Stable Expression of Wild-type and Mutant αIIbβ3 Receptors in Mammalian Cells*—Chinese Hamster Ovary (CHO) cells expressing wild-type (WT) β3 were transfected as described (12) with pcDNA3.1(−)NeoαIIb-R512W, pcDNA3.1(−)NeoαIIb-L841M, or pcDNA3.1(−)NeoαIIb-R512W/L841M to generate the respective cell clones CHO-αIIb(RW)/β3, CHO-αIIb(LM)/β3, and CHO-αIIb(RWLM)/β3. CHO cells expressing WT αIIb were transfected with pcDNA3.1(−)Neoβ3-S527F to generate the CHO-αIIb/β3(SF) cell clone, and CHO-*dhfr*$^+$ cells were cotransfected with pcDNA3.1(−)NeoαIIb-R512W/L841M and pcDNA3.1(−)Neoβ3-S527F to generate the CHO-αIIb(RWLM)/β3(SF) cell clone. Briefly, cells were transfected with DNA using Lipofectamine™ (Invitrogen). Stably transfected cells were obtained by growth in neomycin selection medium (0.7 mg/ml). Colonies were isolated, grown, and analyzed by flow cytometry for expression of αIIb and the β3 polypeptide using anti-αIIb, anti-β3, and anti-αIIbβ3 antibodies. Positive cell populations were enriched by magnetic cell sorting and then subcloned by limiting dilution to obtain 100% positive clones.

*Flow Cytometry*—Surface expression of αIIbβ3 on the transfected cells was analyzed by flow cytometry using anti-human CD41 (anti-αIIb), anti-AP3 (anti-β3), and anti-AP2 (anti-αIIbβ3) monoclonal antibodies as described (12) with some minor modifications. Cells were analyzed on a Coulter Epics XL-MCL flow cytometer (Beckman Coulter, Fullerton, CA).

LIBS expression on αIIbβ3-transfected CHO cells was studied in the presence or absence of RGDS peptide (Sigma). Briefly, washed cells (300,000 cells/μl) were incubated for 30 min at room temperature with or without RGDS (1 mmol/liter), and anti-LIBS monoclonal antibodies or AP2 was added (5 μg/ml) for another 30 min at room temperature. Binding of the anti-LIBS antibodies or AP2 was detected by addition of FITC-labeled rabbit anti-mouse antibodies, and samples were analyzed by flow cytometry as described above.

PAC-1 binding to αIIbβ3-transfected CHO cells was studied in the presence or absence of dithiothreitol (DTT) or anti-LIBS antibodies. CHO cells were washed; resuspended in Iscove's modified Dulbecco's medium with 25 mM HEPES and L-Gln (BioWhittaker, Walkersville, MD); and incubated with 10 mmol/liter DTT (in Iscove's modified Dulbecco's medium with 3.5 mg/ml bovine serum albumin), with 1.1 μg of anti-LIBS antibody, or with Iscove's modified Dulbecco's medium for 20 min at room temperature. Cells were washed with Iscove's modified Dulbecco's medium containing 3.5 mg/ml bovine serum albumin and resuspended in XL buffer (137 mM NaCl, 5 mM KCl, and 50 mM HEPES, pH 7.2), and 1.75 μg of FITC-labeled PAC-1 was added for 45 min at room temperature.

Washed cells were finally resuspended in XL buffer containing 7-aminoactinomycin D and analyzed as described above.

In all flow cytometry experiments, CHO-*dhfr*$^+$ cells were used to gate out the negative population of cells. As a result, a specific mean fluorescence intensity is reported.

*CHO Cell Aggregation*—Cell aggregation was studied as described previously (13). Briefly, transfected CHO cells were washed and incubated with or without 20 mmol/liter DTT for 20 min. Cells were resuspended in Tyrode's buffer incubated with 1 mmol/liter $CaCl_2$ and 0.5 mg/ml fibrinogen for 20 min at room temperature on a horizontal shaker and fixed with 0.5% paraformaldehyde. The presence of cell aggregates was immediately analyzed using a Nikon Eclipse TE200 light microscope. Aggregate size was evaluated by measuring the area covered by each aggregate in one view field (1807 × 1419 μm) using Image Analyzer software (LUCIA, Laboratory Imaging, Analis, Namur, Belgium). The total area covered by all aggregates was calculated and normalized to the total surface measured.

## RESULTS

*Identification of Three New Mutations in the αIIb and β3 Genes of a Patient with an Ill Defined Platelet Disorder*—As the patient was no longer available for further platelet studies, functional analysis of platelets could not be used to identify which platelet receptor is responsible for the platelet disorder. We therefore decided to look for potential genetic defects in platelet receptors and first focused on integrin αIIbβ3, the most abundant platelet receptor with a prominent role in platelet aggregation.

All 30 exons of the αIIb gene and 15 exons of the β3 gene with their intronic splicing signals were amplified by PCR and sequenced. Three new mutations were found, two in the αIIb gene (*ITGA2B*) and one in the β3 gene (*ITGB3*). A C1628T transition in exon 17 of the αIIb gene changed $Arg^{512}$ into Trp (R512W), and a C2615A transversion in exon 26 of the same gene converted $Leu^{841}$ into Met (L841M). A T1657C transition in exon 10 of the β3 gene resulted in a substitution of $Ser^{527}$ with Phe (S527F). Sequence analysis revealed that all mutations in the patient were heterozygous.

*Different Mutant αIIbβ3 Receptors Are Effectively Expressed on the Surface of CHO Cells*—Five CHO cell lines expressing the R512W, L841M, or S527F mutation; both the R512W and L841M mutations; or all three mutations were established: CHO-αIIb(RW)/β3, CHO-αIIb(LM)/β3, CHO-αIIb/β3(SF), CHO-αIIb(RWLM)/β3, and CHO-αIIb(RWLM)/β3(SF), respectively. Surface expression of the mutant receptors on the CHO cell clones was analyzed by flow cytometry using anti-αIIb, anti-β3 (not shown), and anti-αIIbβ3 antibodies (Fig. 1) antibodies. Mock-transfected cells were used as a negative control. Both WT and mutant receptors were effectively expressed on the cell surface (Fig. 1), demonstrating that the introduced mutations did not severely affect expression and translocation to the cell membrane. Expression levels in the different cell lines could not be directly compared in this study because stable cell lines were used. In conclusion, all five cell lines expressed ample αIIbβ3 receptors on their cell surface for further functional analysis. These data are in agreement with the normal αIIbβ3 receptor level expression in the patient's platelets (57,000 receptors *versus* 58,000 in control platelets determined using a platelet glycoprotein IIb/IIIa occupancy kit (Biocytex, Marseille, France)).

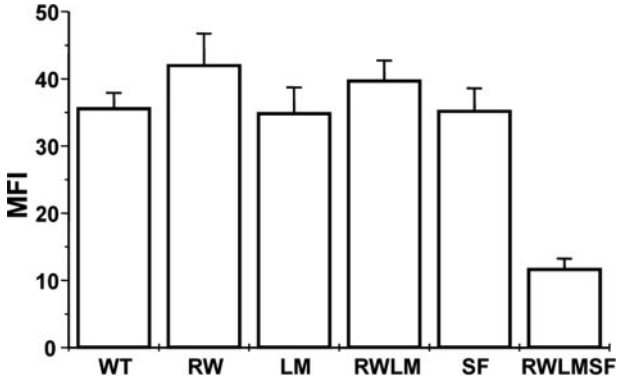


FIGURE 1. **Flow cytometry analysis of WT and mutant αIIbβ3 receptors expressed on CHO cells.** CHO-αIIb(RW)/β3 (*RW*), CHO-αIIb(LM)/β3 (*LM*), CHO-αIIb(RWLM)/β3 (*RWLM*), CHO-αIIb/β3(SF) (*SF*), and CHO-αIIb(RWLM)/β3(SF) (*RWLMSF*) were incubated with 5 μg/ml anti-AP2 antibody (anti-αIIbβ3) for 30 min at 4 °C, and bound antibody was detected by incubation with FITC-labeled rabbit anti-mouse immunoglobulins for another 30 min at 4 °C. Expression was analyzed by flow cytometry. Mean fluorescence intensities (*MFI*) are depicted, and data are the means ± S.D. of 10–23 experiments.

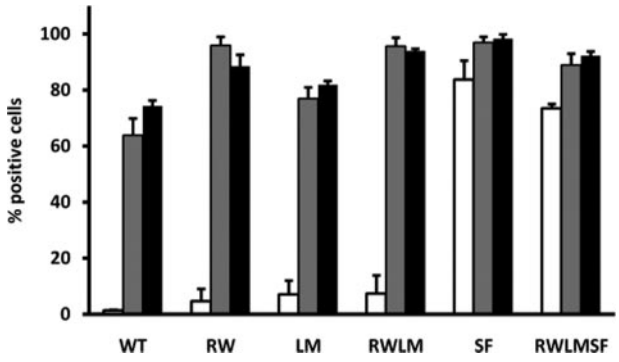


FIGURE 2. **Flow cytometry analysis of PAC-1 binding to WT and mutant αIIbβ3-expressing cells.** Washed CHO cells were incubated without (*white bars*) or with 1.1 μg of anti-LIBS2 antibody (*gray bars*) or 10 mmol/liter DTT (*black bars*) for 20 min at room temperature. FITC-labeled PAC-1 was added for 45 min at room temperature, and bound PAC-1 was assessed by flow cytometry. Data are the means ± S.E. *WT*, CHO-αIIb/β3 ($n$ = 4); *RW*, CHO-αIIb(RW)/β3 ($n$ = 4); *LM*, CHO-αIIb(LM)/β3 ($n$ = 4); *RWLM*, CHO-αIIb(RWLM)/β3 ($n$ = 4); *SF*, CHO-αIIb/β3(SF) ($n$ = 3); *RWLMSF*, CHO-αIIb(RWLM)/β3(SF) ($n$ = 3).

*αIIbβ3 Receptors Carrying the β3 S527F Mutation Spontaneously Bind PAC-1 and Fibrinogen*—To study the competence of the different mutants for ligand binding, we examined the binding of the ligand-mimetic antibody PAC-1 and the ligand fibrinogen to non-activated (low affinity) and activated (high affinity) receptors in the mutant cell lines. Both PAC-1 and fibrinogen are known to interact exclusively with activated αIIbβ3 receptors (10).

As expected, PAC-1 bound poorly to CHO cells expressing WT αIIbβ3 under resting conditions. When αIIbβ3 was activated by addition of DTT (14) or anti-LIBS2 monoclonal antibody (9), PAC-1 bound avidly to these WT receptors (Fig. 2). The same was observed for cell lines expressing mutant αIIbβ3 receptors with only mutations in αIIb (CHO-αIIb(RW)/β3, CHO-αIIb(LM)/β3, and CHO-αIIb(RWLM)/β3) (Fig. 2). Interestingly however, mutant receptors carrying the β3 S527F mutation (CHO-αIIb/β3(SF) and CHO-αIIb(RWLM)/β3(SF))

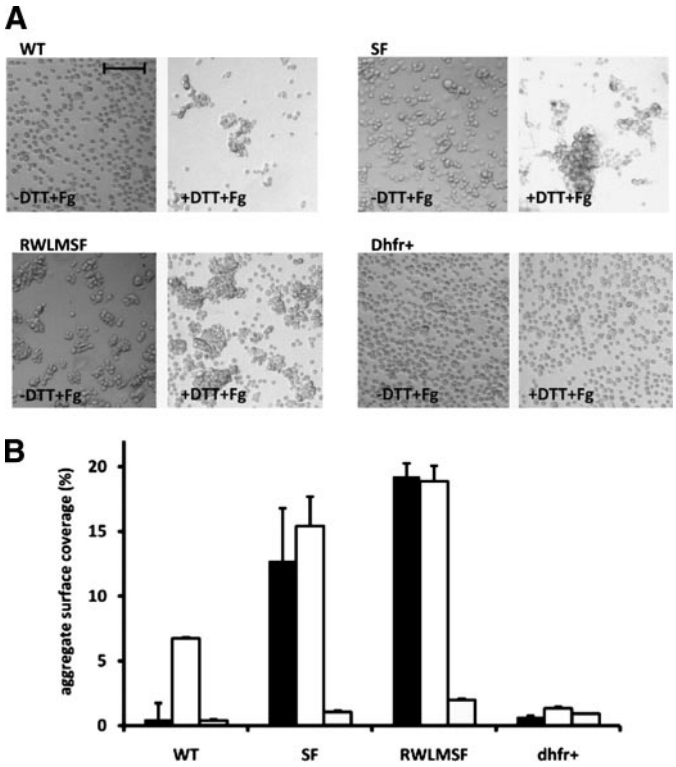


FIGURE 3. **Fibrinogen-induced CHO cell aggregation.** CHO cells expressing WT and mutant αIIbβ3 receptors (CHO-αIIb/β3(SF) (*SF*) and CHO-αIIb(RWLM)/β3(SF) (*RWLMSF*)) and *dhfr*$^+$ cells were washed with Tyrode's buffer and incubated in the presence or absence of DTT for 20 min at room temperature. Cells were resuspended at $3.75 \times 10^6$ cells/ml in Tyrode's buffer containing 1 mmol/liter $CaCl_2$ in the presence or absence of 0.5 mg/ml fibrinogen and were rotated for 20 min. Cells were fixed before analysis. *A*, the images are representative of four individual experiments performed in the presence of both DTT and fibrinogen (*+DTT+Fg*) or in the absence of DTT and presence of fibrinogen (*−DTT+Fg*). *Scale bar* = 100 μm. *B*, shown are the results from quantitative analysis of CHO cell aggregation presented in *A* in the absence of DTT and presence of fibrinogen (*black bars*), in the presence of both DTT and fibrinogen (*white bars*), and in the absence of both DTT and fibrinogen (*gray bars*). The aggregate surface coverage corresponds to the area covered by all aggregates in one view field (1807 × 1419 μm) normalized to the total surface measured. Data are the means ± S.E. of four individual experiments. In each experiment, four view fields were analyzed for each condition.

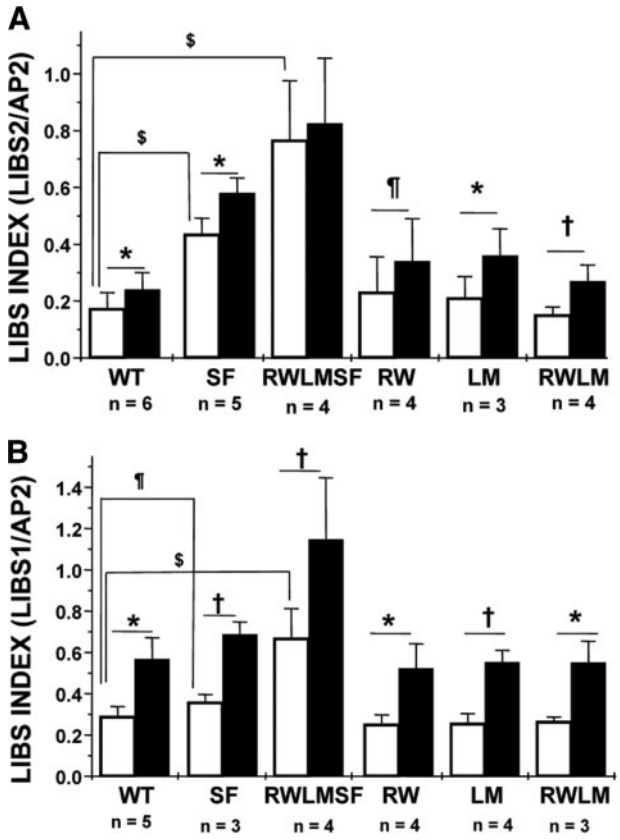


FIGURE 4. **Flow cytometry analysis of LIBS exposure on WT and mutant αIIbβ3 receptors expressed on CHO cells.** Washed cells were incubated for 30 min at room temperature in the absence (*white bars*) or presence (*black bars*) of RGDS peptide. Next, anti-LIBS2 (*A*) or anti-LIBS1 (*B*) antibodies or AP2 (*A* and *B*) was added for 30 min at room temperature, and bound antibody was detected with FITC-labeled rabbit anti-mouse immunoglobulins. Anti-LIBS antibody binding is expressed as the LIBS index, which is the ratio of the mean fluorescence intensity for anti-LIBS antibody (in the presence or absence of RGDS) to the mean fluorescence intensity for AP2. The latter is used for normalization of the amount of receptors expressed on each cell line. Data are the means ± S.D. $, $p < 0.001$; *, $p < 0.01$; †, $p < 0.05$; ¶, $p < 0.1$. *WT*, CHO-αIIb/β3; *SF*, CHO-αIIb/β3(SF); *RWLMSF*, CHO-αIIb(RWLM)/β3(SF); *RW*, CHO-αIIb(RW)/β3; *LM*, CHO-αIIb(LM)/β3; *RWLM*, CHO-αIIb(RWLM)/β3.

spontaneously bound PAC-1 under resting conditions (Fig. 2), demonstrating that these receptors adopt a high affinity conformation.

Interaction of fibrinogen with αIIbβ3 was assessed by performing fibrinogen-induced CHO cell aggregations (13). As expected, under resting conditions, CHO cells expressing WT αIIbβ3 did not aggregate because they were not capable of binding fibrinogen (Fig. 3*A*, *−DTT+Fg*; and Fig. 3*B*, *black bars*). Activation of the WT αIIbβ3 receptors with DTT induced fibrinogen binding and concomitant CHO cell aggregation (Fig. 3*A*, *+DTT+Fg*; and Fig. 3*B*, *white bars*). In contrast, CHO cell aggregation did occur under resting conditions when cell lines expressing receptors carrying the S527F mutation (CHO-αIIb/β3(SF) and CHO-αIIb(RWLM)/β3(SF)) were used (Fig. 3*A*, *−DTT+Fg*; and Fig. 3*B*, *black bars*).

These data indicate that αIIbβ3 receptors carrying the S527F mutation must adopt a high affinity conformation under resting conditions, allowing PAC-1 and fibrinogen binding. This suggests that the S527F mutation disturbs the low affinity conformation of the non-activated receptor and changes it to a constitutively active one.

*LIBS Epitopes Are Exposed in Non-activated αIIbβ3 Receptors Carrying the β3 S527F Mutation*—Ligand-mimetic compounds like RGD peptides induce the extended high affinity conformation of the receptor and LIBS epitope exposure. Studying the expression of LIBS epitopes allows evaluation of the competence of the receptor to bind ligand mimetics and of conformational changes in the receptor. In the absence of RGDS peptide, a significant increase in anti-LIBS2 antibody (9) binding to receptors containing the β3 S527F mutation (CHO-αIIb/β3(SF) and CHO-αIIb(RWLM)/β3(SF)) compared with WT receptors was detected (Fig. 4*A*, *white bars*). This reflects a conformational change in the non-activated S527F receptors. Also the affinity of anti-LIBS1 antibody (8) for receptors carrying the β3 S527F mutation was increased in the absence of RGDS peptide compared with WT receptors (Fig. 4*B*, *white bars*). Addition of RGDS peptide further altered the conformation of these receptors as indicated by a further increase in anti-LIBS monoclonal antibody binding (Fig. 4, *black bars*).

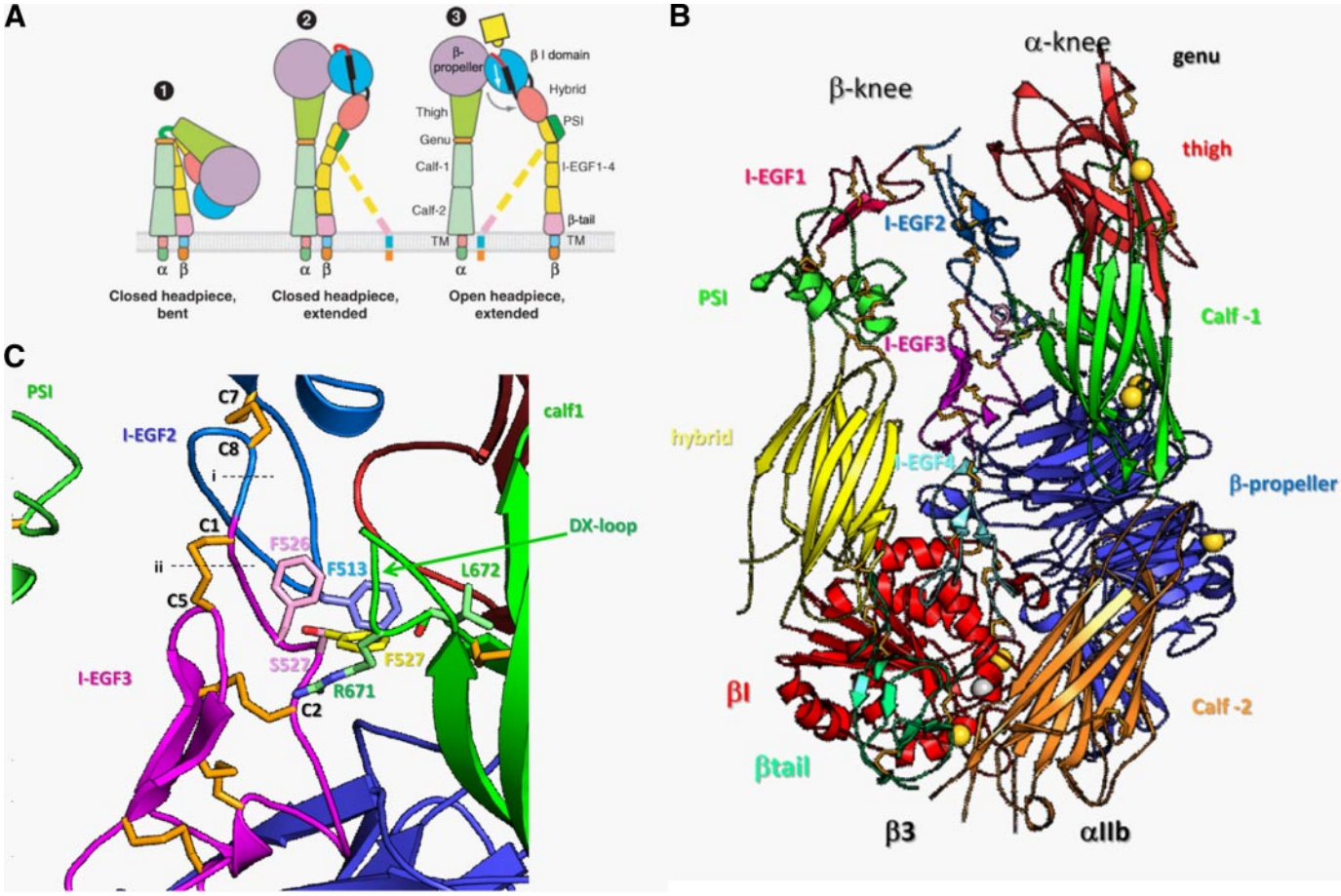


FIGURE 5. **Residue 527 of I-EGF3 is buried in a cleft by the DX loop of the calf-1 domain.** *A*, schematic representation of the organization of the integrin domains in the extended and bent conformations (adapted from Luo *et al.* (2)). *TM*, transmembrane domain. *B*, overall structure of αIIbβ3(6). The ribbon diagram shows most of the αIIbβ3 extracellular domain in its bent conformation. Disulfide bonds are shown in *orange*. Calcium and magnesium ions are shown as *gold* and *silver spheres*, respectively. *C*, region around residue 527 in I-EGF3. Side chains are shown in lighter shades of the colors used for their domains; oxygens are *red*, and nitrogens are *blue*. At residue 527, both the wild-type Ser (*pink*) and mutant Phe (*yellow*) side chains are shown. *Dashed lines* (labeled *i* and *ii*) show the two positions of flexibility at the gimbal-like connection between I-EGF2 and I-EGF3.

The binding of LIBS1 and LIBS2 in the presence or absence of RGDS peptide to all receptors containing mutations only in the αIIb polypeptide chain (CHO-αIIb(RW)/β3, CHO-αIIb(LM)/β3, and CHO-αIIb(RWLM)/β3) was comparable with the binding to the WT receptors (Fig. 4), indicating that these mutations did not alter receptor conformation. In conclusion, these data point out that LIBS epitopes are already expressed in non-activated αIIbβ3 receptors carrying the β3 S527F mutation. The effect of the β3 S527F mutation mirrors a difference in conformation between the mutant and WT receptors.

*Mutation S527F Hinders the αIIbβ3 Receptor from Adopting the Bent Conformation*—In the bent (and thus low affinity) conformation of αIIbβ3, the lower α- and β-legs are in close contact with the headpiece and upper α- and β-legs (6). In this conformation, the lower β-leg (I-EGF2–4 and the tail domain) is buried in a cleft between the upper β-leg (β1, hybrid, PSI, and I-EGF1 domains) and the lower α-leg (calf-1 and calf-2 domains) (Fig. 5*A*). The lower β-leg requires flexibility to enter this cleft, which is occluded by the calf-1 DX loop of αIIb (Fig. 5*B*). Flexibility at interdomain junctions occurs at the gimbal-like or double-jointed connection between the I-EGF domains in the β-leg. The two pivot positions are located (i) in the Cys-*X*-Cys junction between $Cys^8$ of I-EGF2 and $Cys^1$ of I-EGF3 and (ii) in the backbone between $Cys^1$ and $Cys^2$ of I-EGF3 and the $Cys^1$–$Cys^5$ disulfide (Fig. 5*C*, *dashed lines*). Reorientation of the $Cys^1$–$Cys^5$ disulfide bond in I-EGF3 occurs concomitantly with movement of the $Cys^1$–$Cys^2$ loop, which contains residue 527 (Fig. 5*C*) (6).

The side chain of residue 527 in the $Cys^1$–$Cys^2$ loop points toward the DX loop of the calf-1 domain of the αIIb subunit (Fig. 5*B*). Although Phe at position 527 might be accommodated in the cleft, $Phe^{527}$ slightly clashes with $Arg^{671}$ and $Leu^{672}$ in the DX loop. As a consequence, $Phe^{527}$ would hinder entry of I-EGF3 into the cleft and thus prevent αIIbβ3 from adopting the bent conformation. $Phe^{527}$ would not only cause steric hindrance but also reduce flexibility at the gimbal-like connection, which is important for entry of I-EGF3 into the cleft. Because of its larger size and the fact that it can adopt only one of its preferred rotamers, $Phe^{527}$ reduces flexibility of the backbone in the $Cys^1$–$Cys^2$ loop. In summary, the S527F mutation would hinder entry of the I-EGF3 domain into the cleft and adoption of the bent conformation.

## DISCUSSION

Integrins are expressed on the cell surface in a non-activated state not competent for ligand binding. Activation via inside-

out signaling increases the response of the integrins for their ligand. In addition, ligand binding itself transduces signals from the extracellular domain to the cytoplasm in the classical outside-in direction. In this process, two major conformational changes can be observed. One large-scale conformational change occurs upon receptor activation in which the receptor changes from a bent to an extended conformation. In another change, the headpiece, which adopts the closed state in the bent conformation, can adopt either the closed or open state in the extended conformation. The closed and open headpieces have low and high ligand affinities, respectively. Ligand binding induces the extended conformation with the open headpiece. Exposure of LIBS epitopes may occur as a consequence of integrin extension or headpiece opening.

We have demonstrated here that the S527F mutation situated in the I-EGF3 domain of the β3 polypeptide chain induces a high affinity conformation capable of ligand binding without need for prior integrin activation. Indeed, CHO cells expressing the αIIbβ3 receptor containing the β3 S527F mutation spontaneously bind the activation-dependent antibody PAC-1 (Fig. 2) and spontaneously bind fibrinogen, resulting in CHO cell aggregation (Fig. 3). In addition, the conformation of the S527F receptor is altered compared with WT receptors because LIBS epitopes are exposed in the non-activated receptor (Fig. 4). It remains unclear, however, whether the heterozygous S527F mutation is responsible for the mild bleeding phenotype. Indeed, it is expected that a gain-of-function mutation would induce a prothrombotic and not a bleeding phenotype. Interestingly, however, it is known that gain-of-function mutations can cause a bleeding phenotype. Indeed, the rare bleeding disorder "platelet-type von Willebrand disease" is caused by a gain-of-function mutation in the glycoprotein Ibα receptor. These patient platelets have normal glycoprotein Ibα receptor levels and are heterozygous for the mutation. Because we no longer have access to the patient's platelets, we unfortunately cannot support this hypothesis with experimental data. Indeed, the limited laboratory data might also point in the direction of a signal transduction defect such as a $P2Y_{12}$ deficiency.

The S527F mutation is situated in the I-EGF3 domain in the lower β-leg. Mutations inducing constitutively active receptors in I-EGF3 and I-EGF4 have been described. These include the naturally occurring mutations C549R (15), C560R (16), and C598Y (17) and the artificial mutation T562N (18), all of which are gain-of-function mutations. Mutation C598Y induces receptor activation by disrupting the $Cys^{588}$–$Cys^{598}$ bond (17), and it was speculated that replacement of $Cys^{560}$ leads to disulfide bond rearrangement that mimics activation of the integrin (16). Recently, it was demonstrated that the D723H mutation in the β3 polypeptide chain of αIIbβ3 also induces a constitutive, albeit partially activated receptor by disrupting the highly conserved cytoplasmic salt bridge with $Arg^{995}$ in αIIb (19).

The recently published crystal structure of αIIbβ3 (6) shows how mutations in the I-EGF domains in the lower β-leg might induce conformational changes in this receptor. In the bent, low affinity conformation of αIIbβ3, the α- and β-legs bend at their knees to pack the lower legs against the ligand-binding head and upper legs (Fig. 5*A*). The knee in the β-leg is formed by a highly acute bend between I-EGF1 and I-EGF2. The lower β-leg, composed of I-EGF2–4 and the tail domain, has a straight (extended) conformation and is buried in a cleft between the upper β-leg and the lower α-leg in the bent conformation (Fig. 5*A*). Because of the position of the lower β-leg in this cleft, the lower β-leg has far more solvent-accessible surface area (2260 $Å^2$) buried compared with the upper β-leg (1000 $Å^2$), upper α-leg (310 $Å^2$), and lower α-leg (1120 $Å^2$). The extensive burial of the lower β-leg in its cleft between the upper β-leg and lower α-leg makes it particularly susceptible to mutations that cause clashes with neighboring regions of the ectodomain, destabilize the bent conformation, and activate integrins. In addition, the I-EGF domains are small and are dependent on their disulfide bonds for structural stability. As a result, β3 mutations disrupting I-EGF domain disulfide bonds, as in the naturally occurring C560R and C598Y mutations (16, 17), induce conformational changes that might result in receptor activation. Similarly, artificial mutations of most of the cysteines in the β-leg induce receptor activation (20, 21). It has been suggested previously that conformational change (and not a difference in glycosylation) induced by the artificial gain-of-function T562N mutation in the I-EGF4 domain is probably responsible for the activated state of the receptor (18). However, investigation of the crystal structure of the bent αIIbβ3 receptor (6) has shown that the *N*-glycosylation site introduced by the T563N mutation in I-EGF4 is masked by interfaces with the I-EGF3 and hybrid domains and would therefore interfere with burial of the lower integrin β-leg in its cleft (data not shown).

The S527F mutation situated in the I-EGF3 domain also induces conformational changes that result in receptor activation. The S527F mutation is particularly interesting because it is in what is called the gimbal-like or double-jointed connection between I-EGF domains (6). Only a single residue intervenes between the last Cys ($Cys^8$) of one I-EGF domain and the first Cys ($Cys^1$) of the following I-EGF domain. Interdomain movements occur not only at this Cys-*X*-Cys junction between $Cys^8$ and $Cys^1$ but also by flexion of the tip of the following domain, in the backbone between $Cys^1$ and $Cys^2$, and in the disulfide bond between $Cys^1$ and $Cys^5$ (Fig. 5*C*, *dashed lines*). Structural comparisons (6) have demonstrated that the large flexion between the bent and extended orientations of the I-EGF1 and I-EGF2 module pair occurs less in the $Cys^8$-*X*-$Cys^1$ connection and more by flexion of the $Cys^1$–$Cys^2$ loop backbone and $Cys^1$–$Cys^5$ disulfide. Based on comparisons between the bent αIIbβ3 structure and structures of fragments of β2 integrin legs, an overall extended orientation is preferred between I-EGF2 and I-EGF3 (6, 22–24); however, flexibility between I-EGF2 and I-EGF3 is still expected to play an important role in transition between the bent and extended integrin conformations. Because the long axis of I-EGF1 points directly toward the α-knee (Fig. 5*A*), simple extension at the β-knee would result in clashes with the α-subunit. Extension of the integrin knees must be combined with movements at other interdomain junctions to avoid such clashes, and the PSI/I-EGF1 and I-EGF2/I-EGF3 junctions are likely to be the most important junctions for the adjustments during extension and during bending to allow the lower β-leg to dock into its cleft.

The S527F mutation is in the $Cys^1$–$Cys^2$ loop of I-EGF3 (Fig. 5*B*). Among I-EGF domains, the $Cys^1$–$Cys^2$ loop of I-EGF2 is

the longest at 9–13 residues, and the $Cys^1$–$Cys^2$ loop of I-EGF3 is the shortest, with only 4 residues intervening between $Cys^1$ and $Cys^2$. It is hypothesized that longer $Cys^1$–$Cys^2$ loops enable greater gimbal flexibility (6). $Ser^{527}$ is in a region of I-EGF3 that is deeply buried within the cleft between the upper β-leg and lower α-leg of αIIbβ3 (Fig. 5, *B* and *C*). The DX loop of the calf-1 domain bearing $Arg^{671}$ protrudes over this region of I-EGF3 (Fig. 5*C*). Modeling suggests that a Phe residue substituted for $Ser^{527}$ could adopt only one of the four preferred rotamers because the others would clash severely with I-EGF3. If the S527F mutant could adopt the bent conformation, the allowed rotamer would point toward the DX loop (Fig. 5*C*). In the bent conformation, it appears that there may be room for $Phe^{527}$ in the cleft, but only just barely. Among the two independent molecules in αIIbβ3 crystals, the β3 $Phe^{527}$ side chain would either be in close van der Waals contact with or slightly clash with the side chain of $Arg^{671}$ and the carbonyl oxygen of $Leu^{672}$ in the DX loop (Fig. 5*C*).

Therefore, the most plausible explanation for the effect of the S527F mutation is that it would prevent I-EGF3 from entering the cleft and hence prevent αIIbβ3 from adopting the bent conformation. To get past the calf-1 DX loop in entry or exit of the cleft, flexibility at the nearby I-EGF2/I-EGF3 junction appears to be required. Flexibility in the DX loop is limited because the backbone region that includes $Arg^{671}$ is well ordered and rigidified by backbone hydrogen bonds. Clashes of the $Phe^{527}$ side chain with residues including $Arg^{671}$ in the calf-1 domain would hinder entry of I-EGF3 into the cleft. Furthermore, the S527F substitution would decrease flexibility at the gimbal-like connection between I-EGF2 and I-EGF3 by two mechanisms. The much smaller size of the Ser side chain and its ability to access all three rotamers would enable greater backbone flexibility of the $Cys^1$–$Cys^2$ loop than with Phe at position 527. Furthermore, the neighboring β3 $Phe^{526}$ in the $Cys^1$–$Cys^2$ loop of I-EGF3 packs against the $Cys^7$–$Cys^8$ loop of I-EGF2, including $Phe^{513}$. In the mutant, the $Phe^{527}$ side chain is predicted to pack against the other side of $Phe^{526}$, stabilize its interaction with $Phe^{513}$, and hence stabilize the orientation between I-EGF2 and I-EGF3.

In conclusion, the S527F mutation induces a constitutively active receptor enabling spontaneous binding of PAC-1 and fibrinogen and exposure of LIBS epitopes. Insertion of Phe at position 527 in the I-EGF3 domain possibly precludes formation of the bent conformation of αIIbβ3. Indeed, inserting $Phe^{527}$ in the crystal structure of αIIbβ3 reveals that steric hindrance between $Phe^{527}$ and the calf-1 domain and decreased flexibility between I-EGF2 and I-EGF3 may preclude snuggling of I-EGF3 into the cleft and thereby prevent the S527F mutant from adopting a wild type-like bent conformation. The results with the S527F mutation emphasize in WT integrins the importance of the $Cys^1$–$Cys^2$ loops of I-EGF domains in flexibility at the junctions between tandem I-EGF domains and complementarity between the integrin legs in the bent conformation.

*Acknowledgments—We are indebted to Dr. N. Schlegel (Hôpital Robert Debré, Paris), who provided the list of oligonucleotides for amplification of the exons of the αIIb and β3 genes. We thank Dr. M. Ginsberg for the gift of anti-LIBS1 and anti-LIBS2 monoclonal antibodies.*

## REFERENCES

1. Shattil, S. J., and Newman, P. J. (2004) *Blood* **104,** 1606–1615
2. Luo, B. H., Carman, C. V., and Springer, T. A. (2007) *Annu. Rev. Immunol.* **25,** 619–647
3. Ma, Y. Q., Qin, J., and Plow, E. F. (2007) *J. Thromb. Haemost.* **5,** 1345–1352
4. Xiong, J. P., Stehle, T., Diefenbach, B., Zhang, R., Dunker, R., Scott, D. L., Joachimiak, A., Goodman, S. L., and Arnaout, M. A. (2001) *Science* **294,** 339–345
5. Xiong, J. P., Stehle, T., Zhang, R., Joachimiak, A., Frech, M., Goodman, S. L., and Arnaout, M. A. (2002) *Science* **296,** 151–155
6. Zhu, J., Luo, B. H., Xiao, T., Zhang, C., Nishida, N., and Springer, T. A. (2008) *Mol. Cell* **32,** 849–861
7. Xiao, T., Takagi, J., Coller, B. S., Wang, J. H., and Springer, T. A. (2004) *Nature* **432,** 59–67
8. Frelinger, A. L., 3rd, Cohen, I., Plow, E. F., Smith, M. A., Roberts, J., Lam, S. C., and Ginsberg, M. H. (1990) *J. Biol. Chem.* **265,** 6346–6352
9. Frelinger, A. L., 3rd, Du, X. P., Plow, E. F., and Ginsberg, M. H. (1991) *J. Biol. Chem.* **266,** 17106–17111
10. Shattil, S. J., Hoxie, J. A., Cunningham, M., and Brass, L. F. (1985) *J. Biol. Chem.* **260,** 11107–11114
11. Plançon, S., Morel-Kopp, M. C., Schaffner-Reckinger, E., Chen, P., and Kieffer, N. (2001) *Biochem. J.* **357,** 529–536
12. Schaffner-Reckinger, E., Gouon, V., Melchior, C., Plançon, S., and Kieffer, N. (1998) *J. Biol. Chem.* **273,** 12623–12632
13. Morel-Kopp, M. C., Melchior, C., Chen, P., Ammerlaan, W., Lecompte, T., Kaplan, C., and Kieffer, N. (2001) *Thromb. Haemost.* **86,** 1425–1434
14. Zucker, M. B., and Masiello, N. C. (1984) *Thromb. Haemost.* **51,** 119–124
15. Mor-Cohen, R., Rosenberg, N., Peretz, H., Landau, M., Coller, B. S., Awidi, A., and Seligsohn, U. (2007) *Thromb. Haemost.* **98,** 1257–1265
16. Ruiz, C., Liu, C. Y., Sun, Q. H., Sigaud-Fiks, M., Fressinaud, E., Muller, J. Y., Nurden, P., Nurden, A. T., Newman, P. J., and Valentin, N. (2001) *Blood* **98,** 2432–2441
17. Chen, P., Melchior, C., Brons, N. H., Schlegel, N., Caen, J., and Kieffer, N. (2001) *J. Biol. Chem.* **276,** 38628–38635
18. Kashiwagi, H., Tomiyama, Y., Tadokoro, S., Honda, S., Shiraga, M., Mizutani, H., Handa, M., Kurata, Y., Matsuzawa, Y., and Shattil, S. J. (1999) *Blood* **93,** 2559–2568
19. Ghevaert, C., Salsmann, A., Watkins, N. A., Schaffner-Reckinger, E., Rankin, A., Garner, S. F., Stephens, J., Smith, G. A., Debili, N., Vainchenker, W., de Groot, P. G., Huntington, J. A., Laffan, M., Kieffer, N., and Ouwehand, W. H. (2008) *Blood* **111,** 3407–3414
20. Kamata, T., Ambo, H., Puzon-McLaughlin, W., Tieu, K. K., Handa, M., Ikeda, Y., and Takada, Y. (2004) *Biochem. J.* **378,** 1079–1082
21. Mor-Cohen, R., Rosenberg, N., Landau, M., Lahav, J., and Seligsohn, U. (2008) *J. Biol. Chem.* **283,** 19235–19244
22. Beglova, N., Blacklow, S. C., Takagi, J., and Springer, T. A. (2002) *Nat. Struct. Biol.* **9,** 282–287
23. Shi, M., Sundramurthy, K., Liu, B., Tan, S. M., Law, S. K., and Lescar, J. (2005) *J. Biol. Chem.* **280,** 30586–30593
24. Shi, M., Foo, S. Y., Tan, S. M., Mitchell, E. P., Law, S. K., and Lescar, J. (2007) *J. Biol. Chem.* **282,** 30198–30206